Heme oxygenase. Active site structure studied by EPR of cobalt(II) porphyrin-enzyme complex†

Masao Ikeda-Saito,[*1,*2] Hiroshi Fujii,[*3] and Tadashi Yoshida[*4]

[*1] *Department of Physiology and Biophysics, School of Medicine, Case Western Reserve University, USA*

[*2] *Institute for Chemical Reaction Science, Tohoku University*

[*3] *Institute for Molecualr Science*

[*4] *Department of Biochemistry, School of Medicine, Yamagata University*

Structure of the oxygen binding site in the heme complex of heme oxygenase has been elucidated by EPR spectroscopy of cobalt protoporpyrin IX complex of the enzyme. We have found that the bound oxygen is hydrogen-bonded to an amino acid residue in the heme pocket. The hydrogen bonding is favorable to the HO catalytic reaction because by decreasing the reduction potential of oxy HO. The hydrogen bonding also play a role in orienting the bound oxygen for the regiospecific hydroxylation at α-meso-carbon of the porphyrin ring.

Heme oxygenase (HO), an amphipathic microsomal protein, catalyzes the regiospecific oxidative degradation of iron protoporphyrin IX (heme hereafter) to biliverdin, CO, and Fe in the presence of NADPH-cytochrome P450 reductase, which functions as an electron donor.[1–3)] In the catalytic cycle of HO, the enzyme first binds one equivalent of heme resulting in the formation of the heme-enzyme complex, which exhibits optical absorption spectral properties similar to those of myoglobin and hemoglobin. The first electron donated from the reductase reduces the ferric heme iron to the ferrous state, and a molecule of oxygen binds to form a metastable oxy form.[4)] Following the electron donation to the oxy form three stepwise oxygenase reactions are initiated where heme is ultimately converted to the ferric iron-biliverdin complex through α-hydroxyheme and verdoheme intermediates (Fig. 1). Finally, the electron donation from the reductase to the iron-bilverdin complex releases ferrous iron and biliverdin, and the enzyme becomes available for the next turnover. Heme, therefore, participates both as a prosthetic group of the oxygen activation and as a substrate of the enzyme catalysis, a property unique to heme oxygenase. The first monooxygenation cycle of the HO catalysis, where heme is converted to α-meso-hydroxyheme, has been proposed to proceed by reduction of the pseudo-stable O_2-bound complex to a hydroperoxide active intermediate.[5)] This is different from the ferryl-oxo active form of cytochrome P-450 enzymes.[6)] One of the axially coordinated oxygen atoms, presumably the terminal oxygen then attacks the α-meso carbon of the porphyrin ring and hydroxylates it. The structure of the Fe-O_2 unit, a direct precursor of the oxygen activated form, is expected to reflect the distal interactions present in the activated complex. In order to elucidate the active site structure of the oxy form by EPR, we have prepared cobalt(II) prophyrin complex of HO and have conducted EPR measurements. We show here that the bound-O_2 forms hydrogen bond interactions with distal amino acid residues and discuss its implication for the α-meso carbon hydroxylation chemistry.

† This work was supported by NIH grants (M. Ikeda-Saito) and Grants in Aid for Scientific Research from the Ministry of Education, Science, Sports and Culture (H. Fujii and T. Yoshida)

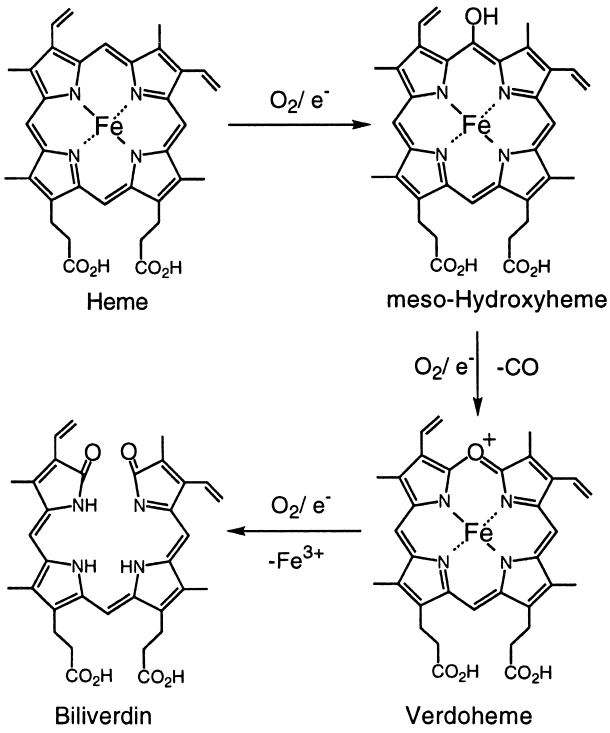

Fig. 1. Reaction intermediates in the heme oxygenase catalyzed oxidation of heme to biliverdinIXα.

Figure 2 illustrates EPR spectra of deoxy forms of cobalt-HO and cobalt-Mb. Deoxy cobalt-HO exhibits an EPR spectrum of axial symmetry that is typical for a five-coordinate cobalt (II) complex with a nitrogenous base axial ligand. The $g_{//}$ signal of deoxy cobalt-HO exhibit an octaplet hyperfine structure due to the hyperfine interaction with ^{59}Co (I = 7/2, 100%) nucleus. Each of the hyperfine lines is further split into triplet by hyperfine interaction with a nitrogen atom (^{14}N; I = 1, 99.6%) of the proximal axial ligand. The g values and hyperfine coupling constants of deoxy cobalt-HO were estimated as $g_{\perp} = 2.310$, $g_{//} = 2.027$, $A_{//}(^{59}\mathrm{Co}) = 8.00$ mT, and $A_{//}(^{14}\mathrm{N}) = 1.80$ mT from a computer EPR simulation (Fig. 2C). The present g values and hyperfine coupling con-

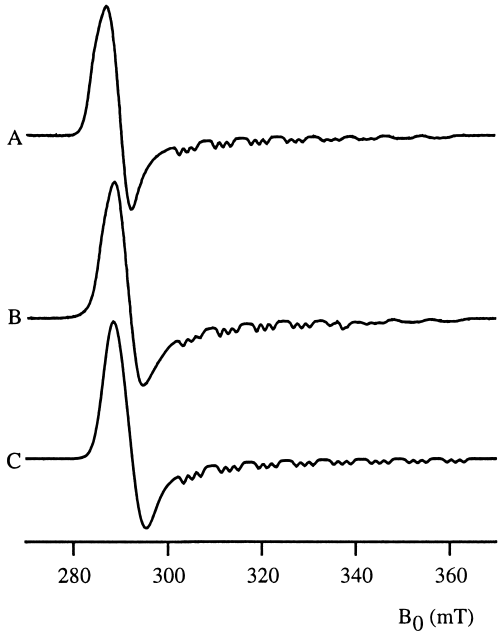

Fig. 2. EPR spectra (20 K) of deoxy cobalt-HO and deoxy cobalt Mb in 0.1 M phosphate buffer, pH 7.0. Conditions: frequency, 9.453 GHz; incident microwave power, 0.10 mW; modulation amplitude at 100 kHz, 0.51 mT. A, deoxy cobalt-Mb. B, deoxy cobalt-HO. C, Computer simulation of (b).

stants of deoxy cobalt-HO are close to those of deoxy cobalt-Mb ($g_{\perp} = 2.327$, $g_{//} = 2.037$, $A_{//}(^{59}\mathrm{Co}) = 7.70$ mT, and $A_{//}(^{14}\mathrm{N}) = 1.67$ mT) that has been characterized a five-coordinate Co(II) state by X-ray crystal crystallography.[7] The axial N-base coordination in deoxy cobalt-HO is consistent with the His25 proximal axial ligand in the heme-HO complex determined in our previous studies.[8]

Figure 3 shows EPR spectra of oxy cobalt-HO and oxy cobalt-Mb. The oxy cobalt-HO exhibits a free radical type spectrum

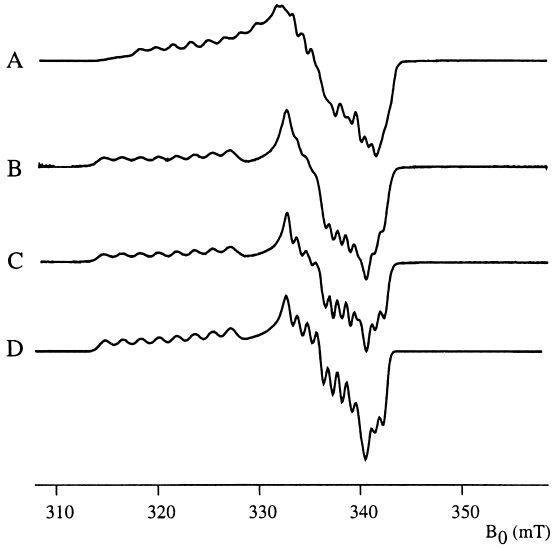

Fig. 3. EPR spectra (20 K) of oxy cobalt-HO and oxy cobalt-Mb in 0.1 M phosphate buffer, pH 7.0. Conditions: frequency, 9.453 GHz; incident microwave power, 0.10 mW; modulation amplitude at 100 kHz, 0.20 mT. A, oxy cobalt Mb. B, oxy cobalt HO. C, oxy cobalt HO in deuterated buffer. D, Computer simulation of B.

centered around $g = 2$ as oxy cobalt-Mb,[9–11] indicating that the O_2 binds to Co(II) in a manner similar to oxy cobalt-Mb.[7] The spectral parameters of oxy cobalt-HO is estimated by computer simulation as $g_1 = 2.104$, $g_2 = 2.007$, $g_3 = 1.990$; $A_1 = 1.76$ mT, $A_2 = 0.98$ mT, $A_3 = 0.83$ mT (Fig. 3D). The oxy cobalt-Mb spectrum has been shown to be composed of at least two species, named type I and II, which are distinct in the distribution of unpaired spin over the dioxygen and in the Co-O_2 bonding geometry.[10] The EPR parameters are: type I, $g_1 = 2.08$, $g_2 = 2.03$, $g_3 = 1.98$; $A_1 = 0.72$ mT, $A_2 = 2.32$ mT, and $A_3 = 0.62$ mT; and type II, $g_1 = 2.085$, $g_2 = 2.008$, $g_3 = 1.983$; $A_1 = 1.73$ mT, $A_2 = 0.82$ mT, and $A_3 = 0.77$ mT.[10] Thus, in contrast to the EPR spectra of the deoxy forms, the EPR spectrum of oxy cobalt-HO is different from that of oxy cobalt-Mb in the following two aspects. First, the g-anisotropy of the cobalt-HO spectrum is different from that of cobalt-Mb. The $g_{//}$ component, g_1, of cobalt-HO spectrum is more anisotropic than that of oxy cobalt-Mb, while the $g_{\perp}$ component, g_2 and g_3, are slightly less anisotropic. This is an indication of different Co-O-O geometry between cobalt-HO and cobalt-Mb, in consistent with the resonance Raman results on the iron couterparts.[12] Second, the spectrum of oxy cobalt-HO consists of a single paramagnetic species, as opposed to the presence of at least two species in oxy cobalt-Mb spectrum which shows the presence of at least two different Co-O-O geometry.[10] The bound dioxygen in oxy cobalt-HO is confined to a well-defined single geometry due to the strong distal pocket interactions as proposed in the resonance Raman studies on the oxy heme-HO complex.[12]

When a paramagnetic ion is surrounded by other ions with nuclear magnetic moments such as protons, there is an appreciable magnetic dipole-dipole interaction between them, which causes line broadening. The linewidth can be reduced by a factor of about one-third by deuteration, because of the smaller nuclear magnetic moment of the deuteron. In a Co^{2+}-O_2 adduct, the paramagnetic center is considered to be the bound O_2.[11] Thus, a reduction of the linewidth in the EPR spectrum of cobalt-MbO_2 is expected upon deuteration, if an exchangeable proton(s) is located near the bound O_2 in oxy cobalt-Mb. Using this D_2O effect on the linewidth of the oxy cobalt EPR spectru,, we have explored possible hydrogen bonding interactions between the bound oxygen and amino acid residues in the distal pocket. The EPR spectrum of oxy cobalt-HO in deuterated phosphate buffer (Fig. 3C) shows significantly sharpened hyperfine structure in comparison to that in H_2O. This indicates that the EPR spectrum of oxy cobalt HO contains the hyperfine coupling with an exchangeable proton that interacts with the bound dioxygen because the line broadening resulting from the hyperfine interaction decreases one-third in going from proton to deuteron. Similar spectral changes have been observed for oxy cobalt-Mb, which is interpreted as evidence for the hydrogen bond formation between the bound dixoygen with the distal histidyl proton by EPR, ESEEM and ENDOR measurements.[13–15] It is likely that a hydrogen bond interaction is present between the bound dioxygen and an amino acid residue in the distal pocket of HO. The presence of a hydrogen bond interaction of the bound dioxygen with distal residues is favorable to the HO catalytic reaction because the interaction of bound dioxygen with proton decreases the reduction potential of oxy HO to form a putative ferric hydroperoxide active species. In fact, when oxy cobalt-HO was reduced by sodium ascorbate

or *p*-hydroquinone, the bound oxygen was reduced to hydrogen peroxide via the cobalt(III) hydroperoxide complex.[16] Furthermore, the hydrogen bond interaction can play a role in orienting the bound oxygen to the position which is favorable to regiospecifically oxidize the α-meso-carbon of the porphyrin ring.

References

1) R. Tenhunen, H. S. Marver, and R. Schmid: J. Biol. Chem. **244**, 6394 (1969).
2) T. Yoshida and G. Kikuchi: J. Biol. Chem. **253**, 4224 (1978).
3) T. Yoshida and G. Kikuchi: J. Biol. Chem. **254**, 4487 (1979).
4) T. Yoshida, M. Noguchi, and G. Kikuchi: J. Biol. Chem. **255**, 4418 (1980).
5) A. Wilks and P. R. Ortiz de Montellano: J. Biol. Chem. **268**, 22357 (1993).
6) M. Sono, M. P. Roach, E. D. Coulter, and J. H. Dawson: Chem. Rev. **96**, 2841 (1996).
7) E. A. Brucker, J. S. Olson, G. N. Phillips, Jr., Y. Dou, and M. Ikeda-Saito: J. Biol. Chem. **271**, 25419 (1996).
8) M. Ito-Maki, K. Ishikawa, K. Mansfield Matera, M. Sato, M. Ikeda-Saito, and T. Yoshida: Arch. Biochem. Biophys. **317**, 253 (1995).
9) J. C. W. Chien and L. C. Dickinson: Proc. Natl. Acad. Sci. USA **69**, 2783 (1972).
10) H. Hori, M. Ikeda-Saito, and T. Yonetani: J. Biol. Chem. **257**, 3636 (1982).
11) B. M. Hoffman and D. H. Petering: Proc. Natl. Acad. Sci. USA **67**, 637 (1970).
12) S. Takahashi, K. Ishikawa, N. Takeuchi, M. Ikeda-Saito, T. Yoshida, and D. L. Rousseau: J. Am. Chem. Soc. **117**, 6002 (1995).
13) M. Ikeda-Saito, R. S. Lutz, D. A. Shelley, E. J. McKelvey, R. Mattera, and H. Hori: J. Biol. Chem. **266**, 23641 (1991).
14) H. C. Lee, J. Peisach, Y. Dou, and M. Ikeda-Saito: Biochemistry **33**, 7609 (1994).
15) M. Höhn and J. Hüttermann: J. Biol. Chem. **257**, 10554 (1982).
16) M.-Y. R. Wang, B. M. Hoffman, and P. F. Hollenberg: J. Biol. Chem. **252**, 6268 (1977).